

Testing for k_T -factorization with inclusive prompt photon production at LHC

A.V. Lipatov, M.A. Malyshev, N.P. Zotov

February 24, 2024

*D.V. Skobeltsyn Institute of Nuclear Physics,
M.V. Lomonosov Moscow State University,
119991 Moscow, Russia*

Abstract

We study the possibility to analyse the data on inclusive prompt photon production at first LHC runs in the framework of the k_T -factorization QCD approach. Our consideration is based on the amplitude for the production of a single photon associated with a quark pair in the fusion of two off-shell gluons. The quark component is taken into account separately using the quark-gluon Compton scattering and quark-antiquark annihilation QCD subprocesses. The unintegrated parton densities in a proton are determined using the Kimber-Martin-Ryskin (KMR) prescription as well as the CCFM evolution equation.

PACS number(s): 12.38.-t, 13.85.-t

The present note is motivated by the very recent measurements [1, 2] performed by the CMS and ATLAS collaborations at the LHC where the isolated photon cross sections have been presented as functions of their transverse momentum at $\sqrt{s} = 7$ TeV for the first time.

The production of prompt photons¹ in hadron-hadron collisions at high energies is a subject of pointed discussions up to now. The theoretical and experimental investigations of such processes provide a direct probe of the hard subprocess dynamics since the produced photons are largely insensitive to the effects of final-state hadronization. The cross sections of these processes are strongly sensitive to the parton (quark and gluon) content of a proton since isolated prompt photons can be produced mainly via quark-gluon Compton scattering or quark-antiquark annihilation (at LO).

We note, however, that a complete theoretical description of the Tevatron data within the QCD is an open question still (see [3, 4] and references therein). It was demonstrated [5, 6] that the overall description of these data in the framework of the standard QCD can be achieved by introducing some additional intrinsic transverse momentum k_T of incoming partons, which is usually assumed to have a Gaussian-like distribution. The average value of this k_T increases from $k_T \sim 1$ GeV to more than $k_T \sim 3$ GeV in hard scattering processes as the \sqrt{s} increases from UA6 to Tevatron energies [5, 7]. The importance of including the gluon emission through the resummation formalism was recognized and only recently this approach has been developed for inclusive prompt photon production [8–11].

In the framework of the k_T -factorization approach of QCD [12], which is of primary consideration in this note, the transverse momentum of incoming partons occurs in a natural way. In this approach, the non-zero partonic k_T is generated perturbatively in the course of non-collinear parton evolution via the corresponding (usually BFKL [13] or CCFM [14]) evolution equations. A detailed description of the k_T -factorization can be found, for example, in reviews [15]. Studies of the prompt photon production at hadronic colliders in the framework of k_T -factorization approach have been done in many papers [16–20]. So, investigations [16–18] have been based on the leading-order matrix elements of quark-gluon Compton scattering and quark-antiquark annihilation subprocesses. An important component of these calculations is the unintegrated (k_T -dependent) quark distributions in a proton. At present, these densities are available in the framework of Kimber-Martin-Ryskin (KMR) [21] approach only since there are some theoretical difficulties in obtaining the quark distributions immediately from CCFM or BFKL equations (see, for example, [15] for more details). In our previous investigations [19, 20] we tried another way. The main idea of [19, 20] was in reexpressing the quark contributions in terms of gluon ones using the higher-order off-shell gluon-gluon fusion matrix elements, namely $g^* + g^* \rightarrow \gamma + q + \bar{q}$. Thus, we reduced the problem of poorly known and poorly calculable unintegrated quark distributions to much better investigated gluon densities. The corresponding contributions from the valence quarks have been taken into account separately. We obtained [19, 20] a reasonably good agreement between the k_T -factorization predictions and the Tevatron data on the inclusive prompt photon production cross sections in both central and forward photon pseudo-rapidity regions. Based on the results [19, 20], in the present note we give the first systematic analysis of data [1, 2] taken by the CMS and ATLAS collaborations at the LHC in the framework of the k_T -factorization approach. Moreover, we improve our previous predictions [19, 20] by

¹Usually the photons are called prompt if they are coupled to the interacting quarks.

taking into account the transverse momentum of incoming off-shell quarks in a proper way. In other aspects we will strictly follow the approach described in [19, 20].

We only briefly recall here the corner-stones of proposed theoretical scheme. The starting point of consideration is the usual leading order $\mathcal{O}(\alpha)$ and $\mathcal{O}(\alpha\alpha_s)$ off-shell subprocesses, namely $q^* + g^* \rightarrow \gamma + q$ and $q^* + \bar{q}^* \rightarrow \gamma + g$. These subprocesses are strongly depend on the unintegrated quark densities in a proton, $f_q(x, \mathbf{k}_T^2, \mu^2)$. The unintegrated quark distributions include the ones of valence quarks $f_q^{(v)}(x, \mathbf{k}_T^2, \mu^2)$, sea quarks appearing at the last step of the gluon evolution $f_q^{(g)}(x, \mathbf{k}_T^2, \mu^2)$ and sea quarks coming from the earlier (second-to-last, third-to-last and other) gluon splittings $f_q^{(s)}(x, \mathbf{k}_T^2, \mu^2)$. In the proposed approach [19, 20] we simulate the last gluon splitting by the higher-order $\mathcal{O}(\alpha\alpha_s^2)$ off-shell matrix elements $g^* + g^* \rightarrow \gamma + q + \bar{q}$. In this way we take into account the contributions from the $f_q^{(g)}(x, \mathbf{k}_T^2, \mu^2)$. To estimate the contributions from the $f_q^{(v)}(x, \mathbf{k}_T^2, \mu^2)$ and $f_q^{(s)}(x, \mathbf{k}_T^2, \mu^2)$ we use the specific properties of the KMR formalism which enables us to discriminate between the various components of the unintegrated quark densities (see below).

Thus, the proposed scheme results to the following partonic subprocesses²:

$$g^* + g^* \rightarrow \gamma + q + \bar{q}, \quad (1)$$

$$q^{*(v,s)} + g^* \rightarrow \gamma + q, \quad (2)$$

$$q^{*(v,s)} + \bar{q}^{*(v,s)} \rightarrow \gamma + g. \quad (3)$$

To be precise, the gluon-gluon fusion (1) takes into account the contribution of the $q^{*(g)} + \bar{q}^{*(g)}$ annihilation subprocesses, and the valence and sea quark-gluon scattering (2) take into account the $q^{*(v)} + \bar{q}^{*(g)}$ and $q^{*(s)} + \bar{q}^{*(g)}$ mechanisms. Evaluation of the off-shell matrix elements of subprocesses (1) — (3) is straightforward and the analytical expressions have been listed in [19]. Here we only would like to mention two technical points. First, according to the k_T -factorization prescription [12], the summation over the incoming off-shell gluon polarizations in (1) and (2) is carried with $\sum \epsilon^\mu \epsilon^\nu = \mathbf{k}_T^\mu \mathbf{k}_T^\nu / \mathbf{k}_T^2$, where \mathbf{k}_T is the gluon transverse momentum. Second, when we calculate the matrix element squared, the spin density matrix for off-shell spinors in (2) and (3) is taken in the form $u(p)\bar{u}(p) = x\hat{p}_p$ [22], where x is the fraction of initial proton longitudinal momentum p_p . In all other respects our calculations follow the standard Feynman rules. Since the expression for the off-shell quark spin density matrix has been derived in the massless approximation, numerically we neglect the charmed quark mass.

According to the k_T -factorization theorem, to calculate the cross section of the prompt photon production one should convolute the off-shell partonic cross sections (1) — (3) with the relevant unintegrated quark and/or gluon distributions in a proton:

$$\sigma = \sum_{i,j=q,g} \int \hat{\sigma}_{ij}^*(x_1, x_2, \mathbf{k}_{1T}^2, \mathbf{k}_{2T}^2) f_i(x_1, \mathbf{k}_{1T}^2, \mu^2) f_j(x_2, \mathbf{k}_{2T}^2, \mu^2) dx_1 dx_2 d\mathbf{k}_{1T}^2 d\mathbf{k}_{2T}^2, \quad (4)$$

where $\hat{\sigma}_{ij}^*(x_1, x_2, \mathbf{k}_{1T}^2, \mathbf{k}_{2T}^2)$ is the relevant partonic cross section. The initial off-shell partons have fractions x_1 and x_2 of initial protons longitudinal momenta and non-zero transverse

²We will neglect the contributions from the so-called fragmentation mechanisms. It is because after applying the isolation cut (see [1, 2]) these contributions amount only to about 10% of the visible cross section. The isolation requirement and additional conditions which preserve our calculations from divergences have been specially discussed in [19, 20].

momenta \mathbf{k}_{1T} and \mathbf{k}_{2T} . The analytical expressions for the contributions of subprocesses (1) — (3) are given in [19].

Concerning the unintegrated parton densities, we use the CCFM-evolved gluon and valence quark distributions derived in [23] and [24], respectively. To determine unintegrated parton densities we also apply the KMR approximation [21]. The KMR approach is the formalism to construct the unintegrated parton distributions $f_a(x, \mathbf{k}_T^2, \mu^2)$ from the known conventional parton distributions $xa(x, \mu^2)$, where $a = g$ or $a = q$. In this approximation, the unintegrated quark and gluon distributions are given by [21]

$$f_q(x, \mathbf{k}_T^2, \mu^2) = T_q(\mathbf{k}_T^2, \mu^2) \frac{\alpha_s(\mathbf{k}_T^2)}{2\pi} \times \int_x^1 dz \left[P_{qq}(z) \frac{x}{z} q\left(\frac{x}{z}, \mathbf{k}_T^2\right) \Theta(\Delta - z) + P_{qg}(z) \frac{x}{z} g\left(\frac{x}{z}, \mathbf{k}_T^2\right) \right], \quad (5)$$

$$f_g(x, \mathbf{k}_T^2, \mu^2) = T_g(\mathbf{k}_T^2, \mu^2) \frac{\alpha_s(\mathbf{k}_T^2)}{2\pi} \times \int_x^1 dz \left[\sum_q P_{gq}(z) \frac{x}{z} q\left(\frac{x}{z}, \mathbf{k}_T^2\right) + P_{gg}(z) \frac{x}{z} g\left(\frac{x}{z}, \mathbf{k}_T^2\right) \Theta(\Delta - z) \right], \quad (6)$$

where $P_{ab}(z)$ are the usual unregulated LO DGLAP splitting functions. The theta functions which appear in (5) and (6) imply the angular-ordering constraint $\Delta = \mu/(\mu + |\mathbf{k}_T|)$ specifically to the last evolution step to regulate the soft gluon singularities. For other evolution steps, the strong ordering in transverse momentum within the DGLAP equations automatically ensures angular ordering³. The Sudakov form factors $T_q(\mathbf{k}_T^2, \mu^2)$ and $T_g(\mathbf{k}_T^2, \mu^2)$ which appears in (5) and (6) enable us to include logarithmic loop corrections to the calculated cross sections.

Note that the function $f_q(x, \mathbf{k}_T^2, \mu^2)$ in (5) represents the total quark distribution function in a proton. Modifying (5) in such a way that only the first term is kept and the second term omitted, we switch the last gluon splitting off, thus excluding the $f_q^{(g)}(x, \mathbf{k}_T^2, \mu^2)$ component. Taking the difference between the quark and antiquark densities we extract the valence quark component $f_q^{(v)}(x, \mathbf{k}_T^2, \mu^2) = f_q(x, \mathbf{k}_T^2, \mu^2) - f_{\bar{q}}(x, \mathbf{k}_T^2, \mu^2)$. Finally, keeping only sea quark in first term of (5) we remove the valence quarks from the evolution ladder. In this way only the $f_q^{(s)}(x, \mathbf{k}_T^2, \mu^2)$ contributions to the $f_q(x, \mathbf{k}_T^2, \mu^2)$ are taken into account.

Other essential parameters were taken as follows: renormalization and factorization scales $\mu = \xi E_T^\gamma$ (where we vary the parameter ξ between 1/2 and 2 about the default value $\xi = 1$ in order to estimate the scale uncertainties of our calculations), LO formula for the strong coupling constant $\alpha_s(\mu^2)$ with $n_f = 4$ massless quark flavours and $\Lambda_{\text{QCD}} = 200$ MeV, such that $\alpha_s(M_Z^2) = 0.1232$. The multidimensional integration in (4) has been performed by means of the Monte Carlo technique, using the routine VEGAS [26]. The full C++ code is available from the authors on request⁴. This code is practically identical to that used in [19, 20] with exception that now we apply it to the LHC conditions.

The results of our calculations are shown in Fig. 1 where we confront the calculated differential cross section of the inclusive isolated prompt photon production (as a function

³Numerically, in (5) and (6) we have applied the Glück-Reya-Vogt (GRV) parton distributions [25].

⁴lipatov@theory.sinp.msu.ru

of the photon transverse energy E_T^γ) with the first LHC data [1, 2] taken by the CMS and ATLAS collaborations at $\sqrt{s} = 7$ TeV. In Fig. 2 we show the data/theory ratio of our predictions. The CMS data refer to the kinematic region defined by $E_T^\gamma > 21$ GeV and $|\eta^\gamma| < 1.45$. The ATLAS data have been measured at $15 < E_T^\gamma < 100$ GeV, $|y^\gamma| < 0.6$, $0.6 < |y^\gamma| < 1.37$ and $1.52 < |y^\gamma| < 1.81$, respectively. In Figs. 1 and 2, the solid and dash-dotted histograms are obtained with the KMR and CCFM parton densities by fixing both the factorization and normalization scales at the default value $\mu = E_T^\gamma$. The upper and lower dashed histograms correspond to the scale variation in KMR predictions as it was described above. One can see that the predictions obtained with the KMR partons tend to slightly overestimate the measured cross sections, but they are coincide with the data within the theoretical uncertainties. Contrary, predictions based on the CCFM evolution lie below the LHC data in a wide E_T^γ range. The main reason of such behaviour is connected with taking into account the contributions from the sea quarks originating from the earlier steps of the evolution cascade in the former case. However, to avoid the possible double counting these contributions are not taken into account in the CCFM calculations since part of them can be already included into the CCFM results (via initial parton distributions which enter to the CCFM equation). Note that the similar effect has been observed [22] in the prompt photon photoproduction at HERA.

The relative contributions of subprocesses (1) — (3) to the prompt photon cross section are shown in Fig. 3. Here we use the KMR parton densities for illustration. One can see that at low E_T the gluon fusion subprocess gives the dominant contribution whereas the QCD Compton and quark-antiquark annihilation subprocesses are mostly significant at higher E_T . The contribution from the quarks appearing from the earlier evolution steps, $f_q^{(s)}(x, \mathbf{k}_T^2, \mu^2)$, is also significant in both central and more forward (as it was measured by the ATLAS collaboration) rapidities.

To conclude, in the present note we apply the CCFM and KMR unintegrated parton densities to the analysis of the first experimental data on the prompt photon production in pp collisions taken by the CMS and ATLAS collaborations at the LHC. We have obtained a reasonably good agreement between our predictions and the LHC data and have demonstrated that the quarks are important even at the LHC energies and therefore should be properly included into the non-collinear evolution equations. It is important for further studies of small- x physics at the LHC, in particular, for investigation of Drell-Yan pair production which give us possibilities to test the region of very low x (up to $x \sim 10^{-5}$).

Acknowledgements. We thank convener of the ATLAS Standard Model Direct Photon working group Marco Delmastro for his interest and very useful remarks. A.V.L and N.P.Z. are very grateful to DESY Directorate for the support in the framework of Moscow — DESY project on Monte-Carlo implementation for HERA — LHC. A.V.L. and M.A.M. were supported in part by the grant of the president of Russian Federation (MK-3977.2011.2). Also this research was supported by the FASI of Russian Federation (grant NS-4142.2010.2) and FASI state contract 02.740.11.0244.

References

- [1] CMS Collaboration, CMS-QCD-10-019, CERN-PH-EP/2010-053; arXiv:1012.0799 [hep-ex].
- [2] ATLAS Collaboration, arXiv:1012.4389 [hep-ex].
- [3] U. Baur *et al.*, "Report of the Working Group on Photon and Weak Boson Production, Batavia 1999, QCD and Weak Boson Physics in Run II"; arXiv:hep-ph/0005226.
- [4] H.-N. Li, Phys. Lett. B **454**, 328 (1999);
T. Binoth, J.Ph. Guillet, E. Pilon, and M. Werlen, Eur. Phys. J. C **16**, 311 (2000);
S. Catani, M. Fontannaz, J.Ph. Guillet, and E. Pilon, JHEP **05**, 028 (2002);
L.E. Gordon and W. Vogelsang, Phys. Rev. D **48**, 3136 (1993).
- [5] L. Apanasevich, C. Balazs, C. Bromberg, J. Huston, A. Maul, W.K. Tung, S. Kuhlmann, J. Owens, M. Begel, T. Ferbel, G. Ginther, P. Slattery, and M. Zielinski, Phys. Rev. D **59**, 074007 (1999).
- [6] H.-L. Lai and H.-N. Li, Phys. Rev. D **58**, 114020 (1998).
- [7] A. Kumar, K. Ranjan, M.K. Jha, A. Bhardwaj, B.M. Sodermark, and R.K. Shivpuri, Phys. Rev. **D68**, 014017 (2003).
- [8] S. Catani, M.L. Mangano, P. Nason, C. Oleari, and W. Vogelsang, JHEP **9903**, 025 (1999).
- [9] N. Kidonakis and J.F. Owens, Phys. Rev. **D61**, 094004 (2000).
- [10] E. Laenen, G. Oderda, and G. Sterman. Phys. Lett. **B438**, 173 (1998).
- [11] E. Laenen, G. Sterman, and W. Vogelsang, Phys. Rev. Lett. **84**, 4296 (2000).
- [12] L.V. Gribov, E.M. Levin, and M.G. Ryskin, Phys. Rep. **100**, 1 (1983);
E.M. Levin, M.G. Ryskin, Yu.M. Shabelsky and A.G. Shuvaev, Sov. J. Nucl. Phys. **53**, 657 (1991);
S. Catani, M. Ciafaloni and F. Hautmann, Nucl. Phys. B **366**, 135 (1991);
J.C. Collins and R.K. Ellis, Nucl. Phys. B **360**, 3 (1991).
- [13] E.A. Kuraev, L.N. Lipatov and V.S. Fadin, Sov. Phys. JETP **44**, 443 (1976);
E.A. Kuraev, L.N. Lipatov and V.S. Fadin, Sov. Phys. JETP **45**, 199 (1977);
I.I. Balitsky and L.N. Lipatov, Sov. J. Nucl. Phys. **28**, 822 (1978).
- [14] M. Ciafaloni, Nucl. Phys. B **296**, 49 (1988);
S. Catani, F. Fiorani and G. Marchesini, Phys. Lett. B **234**, 339 (1990);
S. Catani, F. Fiorani and G. Marchesini, Nucl. Phys. B **336**, 18 (1990);
G. Marchesini, Nucl. Phys. B **445**, 49 (1995).

- [15] B. Andersson *et al.* (Small- x Collaboration), Eur. Phys. J. C **25**, 77 (2002);
 J. Andersen *et al.* (Small- x Collaboration), Eur. Phys. J. C **35**, 67 (2004);
 J. Andersen *et al.* (Small- x Collaboration), Eur. Phys. J. C **48**, 53 (2006).
- [16] M.A. Kimber, A.D. Martin, and M.G. Ryskin, Eur. Phys. J. C **12**, 655 (2000).
- [17] A.V. Lipatov and N.P. Zotov, J. Phys. G **34**, 219 (2007).
- [18] T. Pietrycki and A. Szczurek, Phys. Rev. D **76**, 034003 (2007).
- [19] S.P. Baranov, A.V. Lipatov, and N.P. Zotov, Phys. Rev. D **77**, 074024 (2008).
- [20] A.V. Lipatov and N.P. Zotov, J. Phys. G **36**, 125008 (2009).
- [21] M.A. Kimber, A.D. Martin and M.G. Ryskin, Phys. Rev. D **63**, 114027 (2001);
 G. Watt, A.D. Martin and M.G. Ryskin, Eur. Phys. J. C **31**, 73 (2003).
- [22] A.V. Lipatov and N.P. Zotov, Phys. Rev. D **81**, 094027 (2010).
- [23] H. Jung, arXiv:hep-ph/0411287.
- [24] M. Deak, H. Jung, and K. Kutak, Proceedings of DIS'2008.
- [25] M. Glück, E. Reya and A. Vogt, Z. Phys. C **67**, 433 (1995).
- [26] G.P. Lepage, J. Comput. Phys. **27**, 192 (1978).

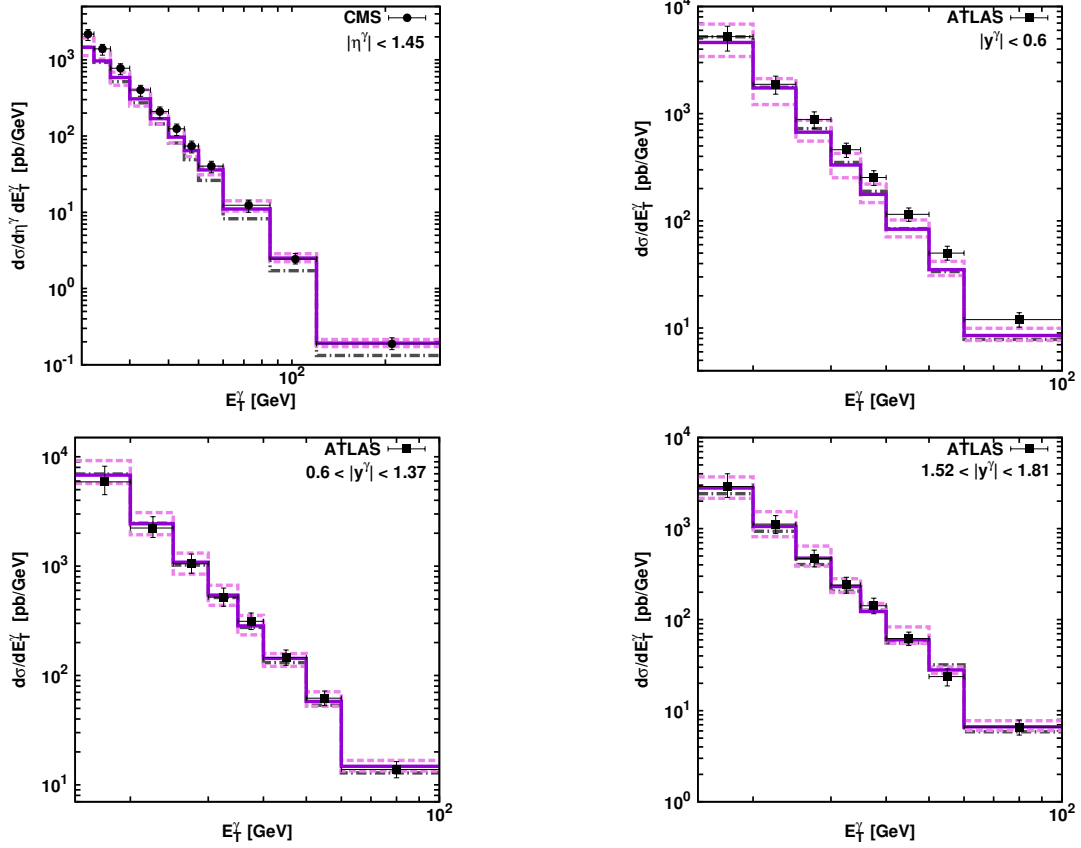


Figure 1: The differential cross sections of the inclusive prompt photon production in pp collisions as a function of E_T^γ calculated at $\sqrt{s} = 7$ TeV. The solid histogram corresponds to the KMR predictions at the default scale $\mu = E_T^\gamma$, whereas the upper and lower dashed histograms correspond to scale variations described in the text. The dash-dotted histogram corresponds to the predictions obtained with the CCFM parton densities. The experimental data are from CMS [1] and ATLAS [2].

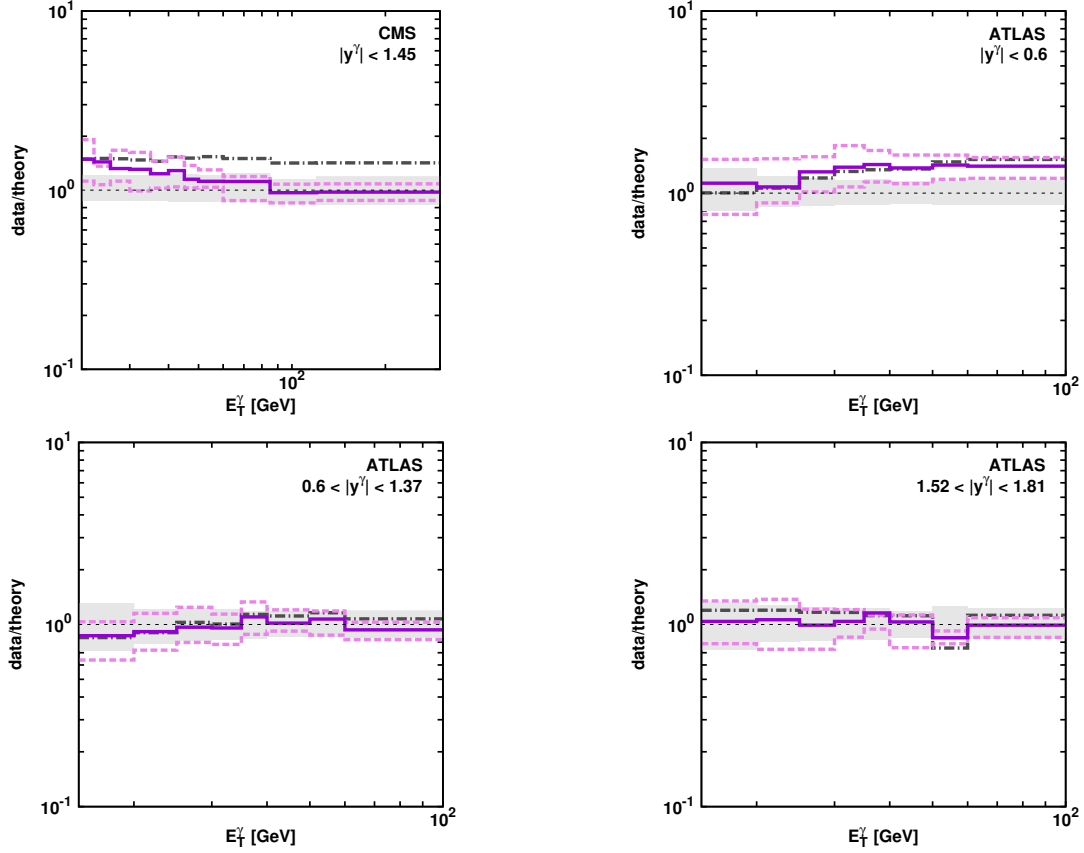


Figure 2: The theory/data ratio of the inclusive prompt photon production in pp collisions as a function of E_T^γ calculated at $\sqrt{s} = 7$ TeV. Notation of the histograms is the same as in Fig. 1. The shaded band represent the experimental uncertainties.

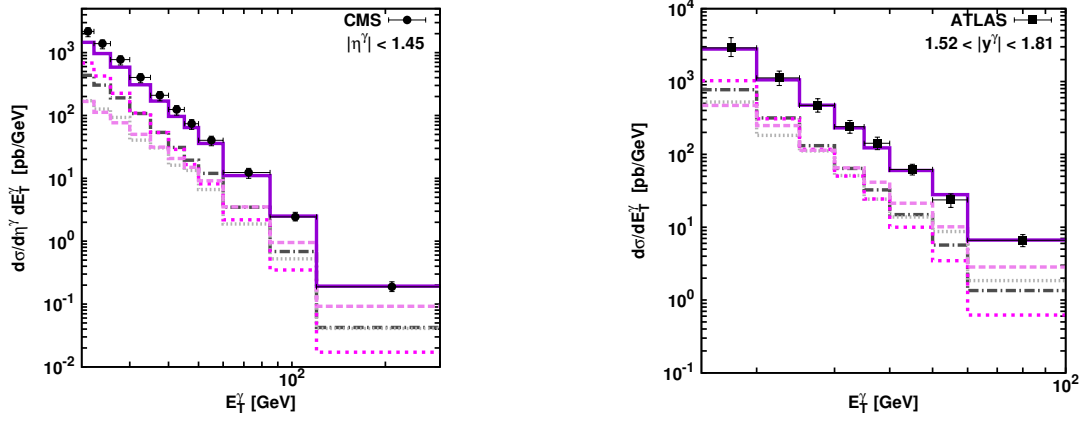


Figure 3: Different contributions to the cross section of the inclusive prompt photon production in pp collisions as a function of E_T^γ calculated at $\sqrt{s} = 7$ TeV. The dashed, short dashed and dotted histograms correspond to the contributions from the $q^*g^* \rightarrow q\gamma$, $g^*g^* \rightarrow q\bar{q}\gamma$ and $q^*\bar{q}^* \rightarrow g\gamma$ subprocesses, respectively. The dash dotted histogram corresponds to the $f_q^{(s)}(x, \mathbf{k}_T^2, \mu^2)$ contribution. The solid histogram represents the sum of all these components. We use the KMR parton densities for illustration. The experimental data are from CMS [1] and ATLAS [2].